A Semi-Active Occupational Shoulder Exoskeleton for Overhead Work With Free Mode and Personalized Assistive Torque

Jin Tian, *Graduate Student Member, IEEE*, Baichun Wei, *Member, IEEE*, Chifu Yang, Haijiao Wang, Feng Jiang, *Senior Member, IEEE*, Hong Huang, Xiang Li, Haiqi Zhu, and Chunzhi Yi, *Member, IEEE*

***Abstract*—Current passive or semi-active shoulder exoskeletons for overhead work provide fixed assistive torque for all participants and tasks, which lacks adaptability. In addition, due to the need to store energy at low elevation angles, they may increase physical demand on the user when assistance is not required. This study presents a novel semi-active shoulder exoskeleton that can provide the free mode (i.e., no assistance) and personalized assistive torque to assist overhead work. The exoskeleton includes the motorized torque generator and hybrid control strategy. The motorized torque generator equipped with servo motor and encoder is characterized by its ability to electrically adjust the peak assistive torque angle and peak torque. In addition, we propose a hybrid control strategy with free and assistive modes. The free mode allows the exoskeleton to not interfere with movements that do not require assistance. The assistive mode provides personalized torque with three levels based on the height and weight of the user. Experimental results validated the exoskeleton's mechanical performance (e.g., high backdrivability) and its assistive effectiveness. The results showed that the exoskeleton could reduce shoulder muscle activation by up to 55.03% and demonstrated a significant difference compared to fixed assistance.**

***Index Terms*—Wearable robotics, musculoskeletal disorders, shoulder exoskeleton, assistive torque, electromyographic signal.**

Received 27 April 2025; accepted 26 October 2025. Date of publication 7 November 2025; date of current version 17 November 2025. This article was recommended for publication by Associate Editor M. Kim and Editor H. Yu upon evaluation of the reviewers' comments. This work was supported in part by the National Key Research and Development Program under Grant 2024YFC3016400, in part by the Ministry of Industry and Information Technology of China, and in part by the Innovation and Transformation Fund Project of Peking University Third Hospital. *(Corresponding authors: Baichun Wei; Chunzhi Yi.)*

This work involved human subjects or animals in its research. Approval of all ethical and experimental procedures and protocols was granted by the Medical Ethics Committee of Harbin Institute of Technology under Application No. HIT-2025028.

Jin Tian, Chifu Yang, Haijiao Wang, and Xiang Li are with the School of Mechatronics Engineering, Harbin Institute of Technology, Harbin 150001, China, and also with the Zhengzhou Research Institute, Harbin Institute of Technology, Zhengzhou 450046, China.

Baichun Wei, Feng Jiang, Haiqi Zhu, and Chunzhi Yi are with the School of Medicine and Health, Harbin Institute of Technology, Harbin 150001, China (e-mail: bcwei@hit.edu.cn; chunzhiyi@hit.edu.cn).

Hong Huang is with the School of Computer Science and Engineering, Sichuan University of Science & Engineering, Yibin 644000, China.

Digital Object Identifier 10.1109/LRA.2025.3630526

I. Introduction

WORK-RELATED musculoskeletal disorders are are a leading cause of health problems among workers worldwide, affecting approximately 1.71 billion people [1]. Among these disorders, shoulder-related conditions are particularly common, accounting for 13% of cases [2]. They frequently result in extended absences from work, with a median duration of 28 days [3], leading to reduced productivity and increased treatment costs. A key risk factor is overhead work, which imposes substantial physical loads and often forces workers into awkward shoulder postures [4]. To address this issue, shoulder exoskeletons have emerged as a cost-effective solution for reducing the risk of injury by supporting the shoulder during overhead tasks [5].

Among these solutions, passive shoulder exoskeletons have seen significant advancements in recent years and have already been implemented in various industrial settings [6]. Unlike their active counterparts, they operate without electronic components, instead storing and releasing elastic potential energy to counterbalance the gravitational torque of the arm. This design enables them to remain lightweight and low-cost. Experimental studies have demonstrated that passive shoulder exoskeletons can effectively reduce muscle activation around the shoulder [7], [8]. However, several key bottlenecks still hinder their widespread adoption.

On the one hand, a major bottleneck is that passive shoulder exoskeletons cannot provide personalized torque, limiting their adaptability to different users and tasks. Currently, they rely on predefined assistive profiles that generate torque as a fixed function of shoulder angle [7]. A fixed shape of torque profile is unlikely to be optimal for all users or task scenarios [9]. Moreover, even for the same task, users with different body sizes may require assistance that deviates from the standard profile [10]. These limitations underscore the need for user-specific torque profiles. Therefore, achieving personalized assistance while preserving the benefits of passive exoskeletons is essential for the adaptability of shoulder exoskeletons.

On the other hand, passive shoulder exoskeletons often require storing elastic energy at low shoulder angles, which can interfere with natural movements such as walking or drinking when the user is not engaged in a task [11]. Despite most passive shoulder exoskeletons allow their assistance magnitude to be adjusted to a low level [12], even the torque at the minimum assistance level may interfere with natural human movements. For example, Exo4Work established a low assistance zone to avoid impeding the user's movements; however, it can only provide a maximum

IEEE Robotics and Automation Letters (RA-L) paper, presented at ICRA 2026, Vienna, Austria. Cite as RA-L paper.

TABLE I
COMPARISON OF SHOULDER EXOSKELETONS

Exoskeleton	Type	W	T	FM	P
Shoulder-sidewinder [17]	Active	6.4 kg	NA	No	No
H-PULSE [14]	Semi-active	5 kg	6 Nm	No	No
Ekso Vest [3]	Passive	4.3 kg	13 Nm	No	No
Exo4Work [18]	Passive	3.8 kg	3 Nm	No	No
Ours	**Semi-active**	**3.75 kg**	**12 Nm**	**Yes**	**Yes**

torque of 3 Nm [13], which may be insufficient for some users and tasks. There is an inherent conflict between delivering high assistance in the overhead region and maintaining low resistance at low shoulder angles, making it difficult to reconcile them both. Therefore, developing an effective solution accommodating high assistance within overhead region and low resistance would further benefit the efficiency of shoulder exoskeleton.

This study presents a novel semi-active shoulder exoskeleton named HIT-SASE for assisting overhead work. Although semi-active shoulder exoskeletons already exist [14], [15], they have not addressed the aforementioned issues and remain limited by fixed torque profiles and the risk of hindering natural movement. Based on the characteristics of the previous exoskeleton HIT-POSE [16], we incorporated motor to adjust the shape of the torque profile (i.e., the peak assistance and peak assistive torque angle), with peak torque personalized according to each user's body characteristics. To enhance the exoskeleton's usability and acceptance, we designed a control strategy featuring two modes. In free mode, the exoskeleton provides no assistance to avoid interfering with natural movement. In assistive mode, the exoskeleton delivers sufficient torque to help the user complete tasks. As shown in Table I, our exoskeleton is the only one that can provide both free mode and personalized assistance simultaneously. The main contributions are as follows.

a) A motorized torque generator is developed to adjust both the angle at which the peak assistive torque occurs (named peak assistive torque angle) and peak torque. To the best of our knowledge, this is the first exoskeleton capable of automatically tuning these two key parameters of the torque profile.
b) The personalized peak assistive torque is determined based on users' height and weight instead of employing a fixed one for all users.
c) A hybrid control strategy with free and assistive modes is designed to address the issue that using elastic elements as a power source may hinder the natural movements.

II. EXOSKELETON DESIGN

A. Design Requirements and System Configuration

Fig. 1 illustrates the scenario of a user wearing the HIT-SASE and its working principle. The back linkage, sliding rail unit, and back panel are secured to the user's body using a waist belt and shoulder straps. A control unit is mounted on the lower back panel. The motorized torque generator, which includes a parallel spring group and a servo motor, is attached to the user's arm via an arm sleeve. Additionally, two rotational degrees of freedom (indicated by green dots in Fig. 1(b)) are incorporated to accommodate natural shoulder movements.

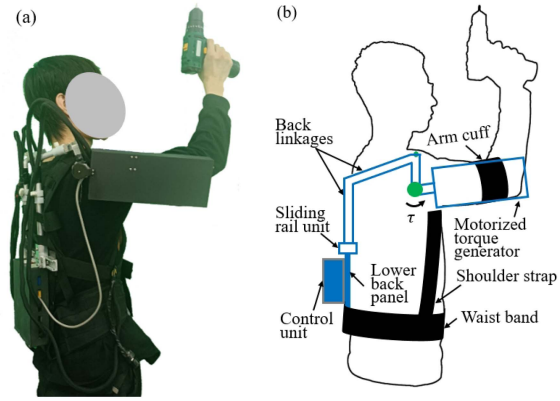

Fig. 1. Scenario of a user wearing the HIT-SASE and its working principle (a) User wearing the HIT-SASE. (b) The working principle. The small and large green dots represent the horizontal and sagittal flexion/extension joints of the exoskeleton, respectively.

The exoskeleton weighs 3.75 kg and is designed to fit users with a back length between 43.6-66.6 cm, and a shoulder width between 29.6–45.6 cm [16]. The control unit with a size of $20 \times 15 \times 5$ cm houses the control board, motor drivers, voltage reduction module, cooling fans, and battery. Specifically, the Raspberry Pi 4B (Rated voltage: 5.1 V) is selected as the control board to communicate with the motor driver (EPOS4 Compact 24/1.5 CAN, Maxon Motor, Sachseln, Switzerland) via serial port and subsequently control the motor. An 8 W brushless motor (EC-max 16, Maxon Motor, Sachseln, Switzerland) drives a ball screw (GP 22S, reduction ratio: 333:1, Maxon Motor, Sachseln, Switzerland) to convert the motor's rotational motion into linear motion of the nut. The motor is equipped with an incremental encoder (Encoder 16 EASY, 1024 CPT, 3 channels, with line driver RS 422, Maxon Motor, Sachseln, Switzerland) to monitor its position. In addition, an incremental encoder (KN35, 1024P/R, Shanghai Heng Xiang Optical Electronics Co.. Ltd., Shanghai, China) is used to measure the shoulder elevation angle. Three switches (one power switch and two mode switches) are employed to activate the system and toggle betwee free and assistive modes. A voltage reduction module steps down the battery's 24 V output to 5.1 V for the Raspberry Pi. All electronic components are powered by a custom-built 3400 mAh lithium battery.

B. Motorized Torque Generator

Fig. 2 shows the components of the motorized torque generator. The pulleys (1 to 3 in Fig. 2), wire rope, and parallel spring group formulate the actuation mechanism. All the design parameters can be found in the previous work [16]. The brushless DC motor is used to adjust both the peak assistive torque angle and the assistance level. When the motor pushes the adjustment rod, Pulley 2 slides along the guide rail, altering the peak assistive torque angle. When the motor pulls the wire rope, the parallel spring group generates a tensile force to assist the shoulder. The user can control the servo motor through a mode switch to select either assistive or free mode. In assistive mode, the servo motor can adjust both the peak assistive torque angle and the assistance level. In free mode, the exoskeleton does not resist arm-lowering movements, allowing natural motion.

IEEE Robotics and Automation Letters (RA-L) paper, presented at ICRA 2026, Vienna, Austria. Cite as RA-L paper.

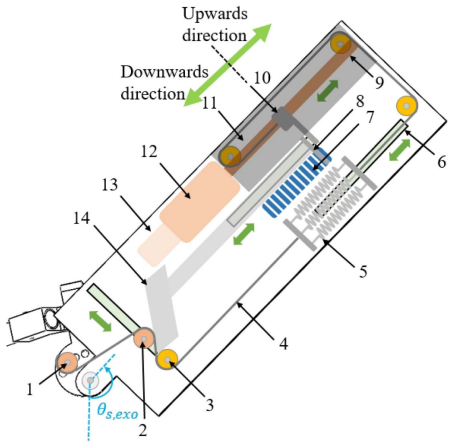

Fig. 2. Schematic diagram of the motorized torque generator with the main components. 1: Pulley fixed on the shoulder bending linkage; 2: Pulley that can move along the guide rail and change the peak assistive torque angle; 3: Pulley used to change the direction of the wire rope; 4: Wire rope; 5: Parallel spring group; 6: Guide rail; 7: Ratchet teeth; 8: Pawl; 9: Ball screw; 10: Ball screw nut with a baffle; 11: Top plane; 12: Brushless DC motor; 13: Motor encoder; 14: Adjustment rod connected to the pawl.

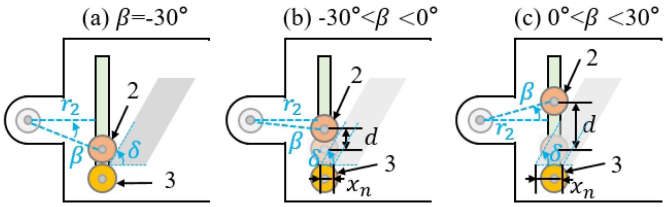

Fig. 3. Schematic diagram of adjusting the peak assistive torque angle.

On the one hand, the motor drives a ball screw nut with a baffle to push down the adjustment rod, which shifts Pulley 2 along the guide rail and adjusts the peak assistive torque angle. The relationship between the peak assistive torque angle and the angle of Pulley 2 (β) can be found in the previous work [16]. Fig. 3 demonstrates the schematic diagram of adjusting the peak assistive torque angle. As shown in Fig. 3(a), the initial position of Pulley 2 corresponds to $\beta = -30°$, while the maximum position reaches $\beta = 30°$. Thus, the displacement of Pulley 2 (d) on the guide rail can be expressed as:

$$d = \begin{cases} r_2(tan(30°) - tan(|\beta|)) & \text{if } -30° \leq \beta \leq 0° \\ r_2(tan(30°) + tan(\beta)) & \text{if } 0° < \beta \leq 30° \end{cases} \quad (1)$$

where r_2 is the distance between the guide rail and the sagittal flexion/extension (F/E) joint (Fig. 1(b)). Therefore, the displacement of the ball screw nut with a baffle (x_n in Fig. 3) can be formulated as:

$$x_n = -\frac{d}{tan(\delta)} \quad (2)$$

where δ denotes the base angle of the parallelogram, x_n here is negative because the nut moves downwards at its initial position (Fig. 2). After that, the adjustment rod connected to the pawl is fixed by the ratchet teeth to ensure that the rod does not return during working process. Then, the user can choose specific assistance level to control the motor.

TABLE II
FIVE LEVELS OF THE MODE SWITCH

Parameter	Value
-1	Adjustment of the Peak Assistive Torque Angle
0	Free Mode
1	Assistive Mode — Low Level
2	Assistive Mode — Medium Level
3	Assistive Mode — High Level

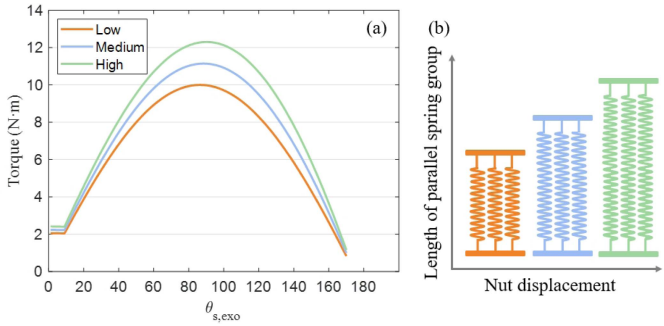

Fig. 4. Different assistance levels of the exoskeleton. (a) An example (with a peak assistive torque angle of 90° and a low-level torque of 10Nm) of torque profiles at different levels. (b) The relationship between nut displacement and the length of parallel spring group.

It is worth noting that adjusting the peak assistive torque angle changes the length of the inner tangent between Pulley 2 and Pulley 3, which in turn affects the extension of the parallel spring group. The change in length of the inner tangent between Pulley 2 and Pulley 3 (l_p) can be determined by

$$l_p = \sqrt{d_c^2 - (R_2 + R_3)^2} \quad (3)$$

$$d_c = d + R_2 + R_3 \quad (4)$$

where d_c denotes the center distance between Pulley 2 and Pulley 3, and $R_2 = R_3$ =7mm indicates their radius.

On the other hand, the ball screw pulls the wire rope in the opposite direction (i.e., upwards in Fig. 2) to adjust the assistance level. The mode switch, which sends commands to the motor, provides five discrete levels, as shown in Table II. The assistive torque at low level is set to 50% of the arm's gravitational torque, with a 6 mm difference in nut displacement between adjacent levels. Fig. 4 illustrates the torque profiles at different assistance levels (with a peak assistive torque angle of 90° and a low-level torque of 10Nm), along with the relationship between nut displacement and the length of the parallel spring group.

The operation process in assistive mode is as follows. First, the user's height and weight are entered to initialize the control program. Second, the mode switch is set to "−1", and the user raises their arms to the target task angle. An incremental encode at the sagittal F/E joint measures the shoulder angle using a 1 s non-overlapping sliding window. If the angle variation within the window (i.e., max–min) is less than 10°, the average value is sent to the controller as the shoulder angle. Only the first valid value is used to drive the motor. After the peak assistive torque angle is set, the user can lower their arms. Third, the user selects the preferred assistance level to perform the task. Finally, once the task is completed, the mode switch is set to "−1", and the user pulls the rope attached to the pawl to reset the adjustment rod. The mode switch is then set to "0".

TABLE III
DISCRETE TORQUE TRACKING PERFORMANCE

No	W [kg]	H [m]	τ_d [Nm]	τ_a [Nm]
1	85	1.75	6.30	6.07
2	66	1.88	5.26	5.24
3	65	1.65	4.55	4.68
4	68	1.70	4.90	5.30
5	77	1.75	5.71	5.92
Mean±Std	72.2 ± 8.6	1.75 ± 0.09	5.34 ± 0.69	5.44 ± 0.56

TABLE IV
DIFFERENT CONDITIONS IN EXPERIMENTS

No	Conditions
1	NO EXO
2	EXO Free
3	EXO Low
4	EXO Medium
5	EXO High
6	EXO Fixed_Low
7	EXO Fixed_Medium
8	EXO Fixed_High

C. Hybrid Control Strategy

1) Human Shoulder Biomechanics: The shoulder torque (τ_s) can be derived from equation (5).

$$\tau_s = I(\theta)\ddot{\theta} + C(\theta, \dot{\theta}) + G(\theta) \tag{5}$$

where θ is the sagittal F/E angle of the shoulder, $I(\theta)$ denotes the moment of inertia of the human arm, $C(\theta, \dot{\theta})$ is the Coriolis and centrifugal torque of the human arm. Since overhead tasks are typically quasi-static, the shoulder joint torque is primarily influenced by gravitational forces [19]. Then the estimated shoulder joint torque ($\hat{\tau}$) can be expressed by a quasi-static model, as shown in equation (6).

$$\hat{\tau} = m_{arm} g l_{arm} sin(\theta) \tag{6}$$

where m_{arm} is the weight of the arm, l_{arm} is the distance from the shoulder joint to the arm's center of mass. Both parameters can be estimated based on individual's weight and height [20]. $\hat{\tau}$ reaches its maximum value when $\theta = 90°$. The desired assistive torque at the low level (τ) was defined as equation (7).

$$\tau = k\hat{\tau} \tag{7}$$

where k is a positive constant, representing the percentage of shoulder joint torque. In this article, we defined k as 0.5 [21]. Here, τ is used to determine the peak assistive torque, i.e., $\hat{\tau}$ is the value when $\theta = 90°$. The assistive torque profile is determined by the structural configuration of the exoskeleton. To obtain the desired assistive torque, the user's height and weight are input into the control system, which then uses equations (6) to(7) to compute the desired torque and accordingly control the motor behavior.

2) Description of the Assistive Torque: The relationship between the motor rotation angle (θ_m) and the ball screw nut displacement (x_n) at the low assistance level can be derived from equation (8).

$$x_n = \frac{p}{2\pi}\theta_m \tag{8}$$

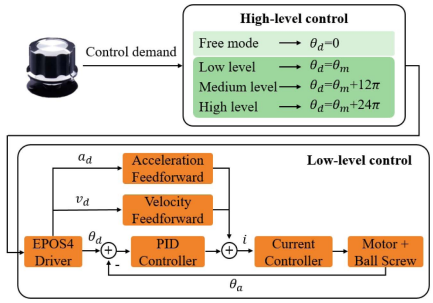

Fig. 5. Control system of the exoskeleton. The control demand can be manually input through switches; the green part represents the assistive mode; θ_d and θ_a denotes the desired and actual rotation angle of the motor; a_d and v_d is the required acceleration and velocity; i represents the current demand value.

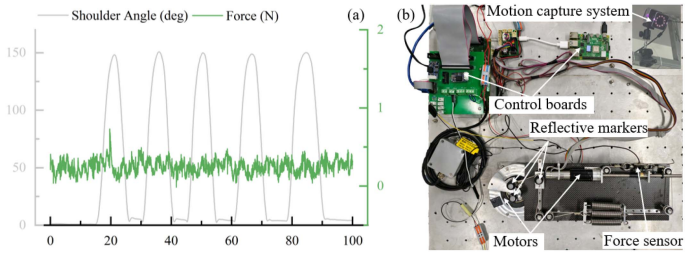

Fig. 6. (a) The result of the mechanical resistance characterization in free mode. (b) The test bench setup in torque tracking.

where p is the pitch of the ball screw, equal to 1mm. The spring force generated (F_s) is determined by x_n, the change in the inner tangent length between Pulley 2 and Pulley 3 (l_p), and the spring's initial tension length (l_0), as shown in equation (9).

$$F_s = K(x_n + l_0 + l_p) = \frac{\tau}{r} \tag{9}$$

where r is the force arm corresponding to the peak assistive torque angle, K is the stiffness of the parallel spring group, equal to 12N/mm, and τ denotes the desired assistive torque, determined by equation (7). l_0 is used to prevent the wire rope from loosening, which is equal to 5mm. Based on equations (8) to(9) , the relationship between θ_m and τ can be expressed as equation (10).

$$\theta_m = \frac{p}{2\pi}\left(\frac{\tau}{rK} - l_0 - l_p\right). \tag{10}$$

Here, θ_m denotes the motor rotation angle at the low assistance level. To reach the medium level, the motor must rotate an additional 6 turns (i.e., 6*2π*1=12π). Another 6 turns are required to reach the high level.

3) Control System: As shown in Fig. 5, the control system consists of a high-level and a low-level controller. The high-level controller includes four modes: one free mode and three assistive modes (i.e., low, medium, and high), which are selected via a mode switch. The low-level controller uses a position control loop implemented with a PID controller. To enhance tracking performance, feedforward control based on acceleration and velocity is added to the position regulation.

IEEE Robotics and Automation Letters (RA-L) paper, presented at ICRA 2026, Vienna, Austria. Cite as RA-L paper.

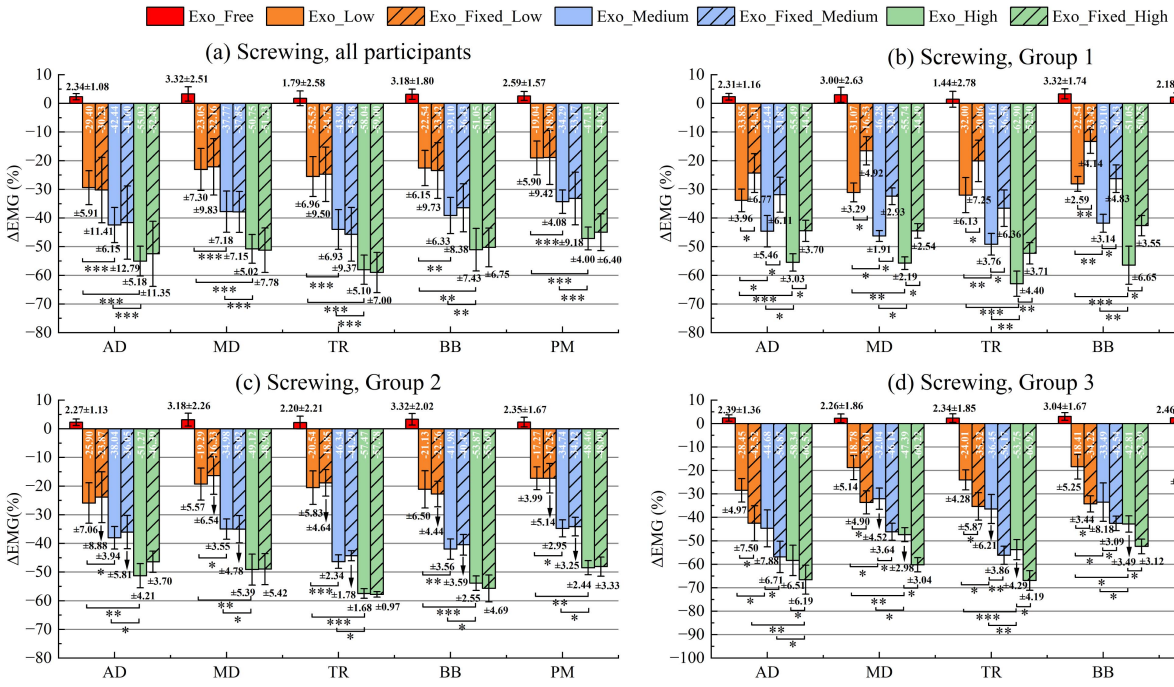

Fig. 7. Statistical results (mean± standard error) of EMG on screwing task from pairwise comparisons. (a) All participants. (b) Group 1. (c) Group 2. (d) Group 3. Negative values mean reduced EMG activity with respect to the NO EXO condition. Except for EXO Free condition, all EXO conditions are significantly different from the NO EXO condition. *: $p < 0.05$; **: $p < 0.01$; ***: $p < 0.001$.

III. Experiments and Results

A. Backdrivability in Free Mode

To characterize the backdrivability in the free mode, we measured the mechanical resistance (i.e., backdrivability force) during shoulder flexion and extension using a force sensor (T313, Changzhou Right Measurement and Control System Co., Ltd.) in series with the parallel spring group. Due to the lower elastic potential energy stored in the parallel spring group at low joint angles, the exoskeleton generated very low resistance, with a peak backdrivability force of 0.73 N and an average absolute resistance of 0.25 N (Fig. 6(a)). This is significantly lower than that in [18], where the minimum value was 44 N and the maximum was 103.4 N.

B. Discrete Torque and Position Tracking

Since the motor adjusts the assistance level by sending discrete commands, we evaluated the torque and position tracking performance under discrete control inputs. The desired peak assistive torque (τ_d) was calculated using equations (6) to (7) and five participants' anthropometrics (Table III). Based on this value, the motor generated corresponding displacement commands to adjust the spring length. The actual peak assistive torque (τ_a) during the flexion-extension process was then measured on the test bench using the motion capture system and force sensor (Fig. 6(b)). The tracking performance is shown in Table III. The absolute difference between the desired (5.34 ± 0.69 Nm) and actual (5.44 ± 0.56 Nm) peak assistive torques was 0.20 ± 0.14 Nm (mean $\pm$ std). This indicates that the exoskeleton can provide personalized torque for different users.

The desired position (p_d) was set to 6mm and converted into the corresponding motor position command. The actual position (p_a) was defined as the displacement of the nut along the ball screw. We tested ten times on the test bench and the difference between the desired and actual positions was 5.9680 $\pm$ 0.2622mm (mean $\pm$ std). This indicates that the mechanical system has good tracking performance, ensuring that the motor can accurately switch between assistance levels.

C. Efficiency

We evaluated the efficiency of motor output transmission to the parallel spring group at a shoulder flexion angle of 90°, which corresponds to the exoskeleton's primary usage scenario and target position. The power consumed (P_{input}) can be calculated as an integral of output force over displacement:

$$P_{\text{input}} = \int f \, d(\Delta L) \tag{11}$$

where f is the output force by the screw, and ΔL is the corresponding displacement of the nut. The power delivered (P_{output}) can be obtained through the elastic potential energy of the parallel spring group:

$$P_{\text{output}} = \frac{1}{2} K (\Delta x)^2 \tag{12}$$

where K is the stiffness of the parallel spring group, and Δx is its extension length. The efficiency is defined as:

$$\eta = \frac{P_{\text{output}}}{P_{\text{input}}} \times 100\% \tag{13}$$

We recorded the parameters defined in equations (12) to (13) during five transitions from the low to medium level. The efficiency was from a minimum of 75.89% to a maximum of 85.35%, and the average was 81.21 $\pm$ 3.92%.

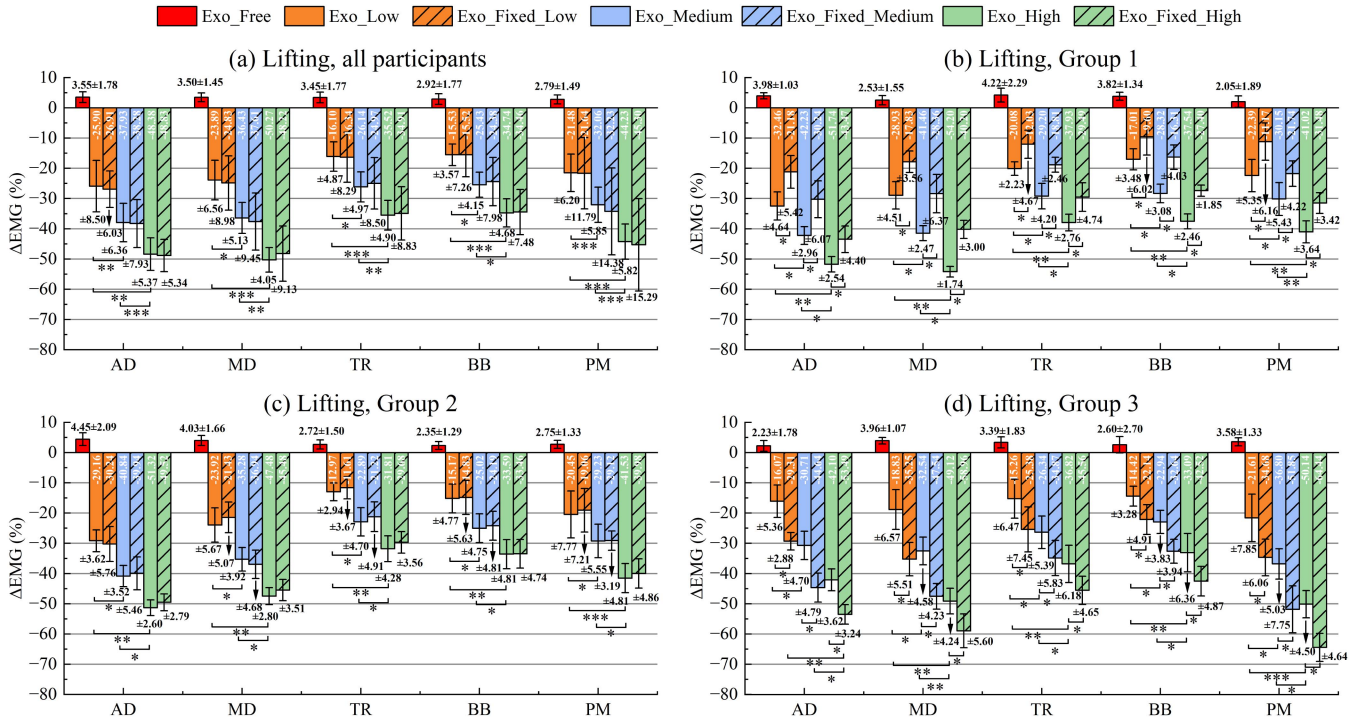

Fig. 8. Statistical results (mean± standard error) of EMG on lifting task from pairwise comparisons. (a) All participants. (b) Group 1. (c) Group 2. (d) Group 3. Negative values mean reduced EMG activity with respect to the NO EXO condition. Except for EXO Free condition, all EXO conditions are significantly different from the NO EXO condition. *: $p < 0.05$; **: $p < 0.01$; ***: $p < 0.001$.

D. Response Time

The response time for transitions between free and assistive modes is critical to the practical usability of the exoskeleton. The response time was defined as the duration between the mode switch sending a command and the motor receiving it. Ten cycles were performed, each consisting of a transition from free to assistive mode and back, to measure the response time. The results showed that the average response time was 73.72 ± 36.68ms, with 102.22 ± 14.11ms for the transition from free to assistive mode and 45.22 ± 28.84ms for the reverse transition.

E. Power Consumption

The power consumption is directly related to the exoskeleton's sustainable operating time. The motor's power consumption was defined as the product of its current and voltage. The power capacity of the battery is 81.6Wh. We recorded the motor current and voltage during a single assistance level transition, and the corresponding power consumption was 1.2W. Consequently, the battery can power two motors running for up to 34 hours, which is sufficient for an 8-hour workday.

F. System Performance Evaluation

To evaluate the system's performance in overhead tasks, we conducted experiments analyzing muscle activation under eight different conditions (Table IV). A fixed low-level assistance was set to 50% of the arm's gravitational torque for an individual of 170cm height and 70kg weight [21], [22].

1) Experimental Protocol: All experimental protocol received approval from the Medical Ethics Committee of Harbin Institute of Technology (HIT-2025028). Nine health participants (males, one left-handed, age 23.4 ± 2.1 years, weight 70.3 ± 11.0kg, height 170.9 ± 7.6cm) signed consents before experiments. The participants were given 30 minutes to familiarize themselves with the exoskeleton. According to the weights and heights of all participants, we divided them into three groups, with three people in each group: Group 1 (the height was not lower than 175cm and the weight was not lower than 75kg); Group 2 (the height was 170 ± 5cm and the height was 70 ± 5kg); and Group 3 (the height was not higher than 165cm and the weight was not higher than 65kg). We selected height and weight as the criteria for classifying the participants because the peak assistive torque of the exoskeleton was determined based on these parameters, as shown in equation (6). In Group 1, the personalized assistance was greater than fixed assistance in the same level; in Group 2, the former was comparable with the latter; in Group 3, the former was lower than the latter.

The first task was one-handed screwing using a 207g electric wrench to fasten 25 loosely inserted M5 bolts at shoulder height. The second task was two-handed lifting, where participants held a 5kg load at a shoulder and elbow angle of 90° for 15 seconds. In both tasks, static postures were maintained before and after execution. The two tasks were performed once under eight conditions, and the tasks and conditions were in a random order.

2) Data Analysis: Surface electromyography (EMG) signals of five muscles were collected bilaterally using EMG electrodes (1111Hz, Delsys Inc., Natick, MA, USA) according to SENIAM guidelines [23]: anterior deltoid (AD), middle deltoid (MD), trapezius (TR), bicep brachii (BB), and pectoralis major (PM). AD and MD are responsible for the movement and stabilization of the humerus and are expected to directly benefit from the exoskeleton [12]. TR plays a key role in scapular rotation and

IEEE Robotics and Automation Letters (RA-L) paper, presented at ICRA 2026, Vienna, Austria. Cite as RA-L paper.

translation [8]. BB crosses the shoulder joint and assists AD in producing shoulder flexion [24]. PM contributes to shoulder flexion and works synergistically with AD to generate adduction torque, thereby helping stabilize the shoulder [15]. Antagonistic muscles, such as the triceps brachii, were not included because they are not primary load-bearing muscles during overhead tasks [18]. Additionally, deep stabilizing muscles like the rotator cuff were excluded from the EMG analysis due to the difficulty of monitoring them directly using surface electromyography [25]. Maximal voluntary contraction of each muscle was measured prior to the experiment for normalization. After EMG preprocessing, the root mean square (RMS) of each muscle was obtained from the linear envelope via a 100ms time sliding window during the task execution phase. Finally, the percentage variation with respect to the NO EXO condition (ΔEMG) was computed according to equation (14) [14].

$$\Delta EMG(\%) = \frac{EMG_{RMS}^{EXO} - EMG_{RMS}^{NOEXO}}{EMG_{RMS}^{NOEXO}} \tag{14}$$

where EMG_{RMS}^{EXO} is the RMS under one of EXO conditions, and $EMG_{RMS}^{NOEXO}$is the RMS under the NO EXO condition. We calculated the results of dominant side across participants for screwing task, and the results of left and right sides were averaged across participants for lifting task. The Shapiro-Wilk test was employed to check data normality. The analysis of variance (ANOVA) was conducted to check for across-condition differences. A post-hoc analysis was conducted when a significant effect was observed. Statistical significance was concluded when p<0.05.

3) Results: In terms of screwing task of all participants, statistically significant interactions were found in all monitored muscles (AD: $\chi^2(7) = 57.3$, p<0.001; MD: $F(7,64) = 26.3$, p<0.001; TR: $\chi^2(7) = 57.9$, p<0.001; BB: $\chi^2(7) = 57.7$, p<0.001; PM: $F(7,64)= 44.0$, p<0.001). Similarly, for lifting task, there were statistically significant interactions in AD ($\chi^2(7)$=55.74, p<0.001), MD ($F(7,64) = 56.05$, p<0.001), TR ($\chi^2(7) = 58.37$, p<0.001), BB ($F(7,64) = 20.73$, p<0.001), and PM ($\chi^2(7)$=57.85, p<0.001) among all participants. For both screwing and lifting tasks, as shown in Figs. 7 and 8, in all groups (i.e., all participants, Group 1, Group 2, and Group 3), the AD, MD, TR, BB, and PM muscles exhibited significantly decreased EMG activations in all EXO conditions (expect for EXO Free) with respect to NO EXO; there were also significant differences between EXO Low, EXO Medium, and EXO High. The monitored muscles exhibited no significantly differences in results of all participants and Group 2 between EXO Low and EXO Fixed_Low, EXO Medium and EXO Fixed_Medium, EXO High and EXO Fixed_High, but the significant differences were found in results of Group 1 and Group 3. The highest reduction among participants in screwing task was up to 55.03% for AD, and that in lifting task was up to 50.27% for MD.

IV. Discussion

A. Characterization of the Mechanical Performance

We conducted bench tests to evaluate the exoskeleton's mechanical performance, including backdrivability in free mode, discrete torque and position tracking, efficiency, response time, and power consumption. In free mode, the exoskeleton demonstrated excellent backdrivability, with a peak resistance of 0.73 N. Additional results showed that the mechanical system is capable of providing effective assistance and holds promise for real-world applications.

B. Effects of the Exoskeleton in Different Assistance Levels

We recorded the activations of muscles involved in shoulder movement and stabilization to assess the exoskeleton's effects across two tasks under eight conditions. Results showed that HIT-SASE significantly reduced muscle activation in both tasks (Figs. 7 and 8), suggesting its potential to alleviate fatigue and assist various types of overhead work, consistent with previous studies [15], [24]. Compared to NO EXO, muscle activations under EXO Free showed no significant increase, supporting the effectiveness of the free mode and indicating a reasonably balanced mass distribution. As expected, the degree of EMG reduction correlated with the assistance level, likely due to increased assistive torque [14].

In all participants, when the assistance levels were the same, there were no statistically significant differences between personalized and fixed assistances (Fig. 7(a) and 8(a)). It is likely due to the existence of Group 2, where the same level of the two assistance (i.e., personalized and fixed) were essentially identical. In addition, when the assistance levels were consistent between personalized and fixed assistances, we found significant difference in Groups 1 and 3 (Fig. 7(b) and (d) , Fig. 8(b) and (d) . Especially in Group 1, the EMG reductions in personalized assistances were greater. These results indicate that the personalized assistance was functional and effective, and the exoskeleton with personalized assistance could accommodate a wider range of users.

Furthermore, for both tasks, the condition with the highest EMG reduction in Group 3 was EXO Fixed_High. This may be explained by the greatest assistance (about 75% of the arm's gravity torque) in EXO Fixed_High, which is consistent with previous studies [14], [16]. However, this assistance may lead to a potential increase in antagonistic muscle activation (such as triceps brachii) [26], especially for individuals with lower height and weight (such as participants in Group 3). The minimum assistance provided by the fixed assistance scheme to Group 3 is also greater than 50% of the arm's gravity torque. Similarly, the maximum assistance provided by the fixed assistance scheme to Group 1 is less than that of the personalized assistance. This could limit the range of assistance options of users and may further reduce the user acceptance and overall usability of the exoskeleton.

C. Limitations

Despite the positive results, our study still contains some limitations. First, the number of participants in different group (i.e., Group 1, Group 2, and Group 3) was relatively small. Next, we plan to invite more participants to experience this exoskeleton. Secondly, the peak assistive torque angle can only be adjusted once in a task, which could reduce the performance of the exoskeleton in more complex overhead tasks. Finally, in assistive mode, the exoskeleton still resists arm lowering. In the future, we will use sensors (e.g., IMUs) to detect this phase and switch to free mode.

V. Conclusion and Future Work

This article presents a novel semi-active shoulder exoskeleton named HIT-SASE to provide assistance for overhead work. The

IEEE Robotics and Automation Letters (RA-L) paper, presented at ICRA 2026, Vienna, Austria. Cite as RA-L paper.

exoskeleton is characterized by the free mode (i.e., no assistance) and personalized assistance. First, the motorized torque generator equipped with servo motor and encoder is developed to automatically adjust the peak assistance and the peak assistive torque angle. Second, we deploy the hybrid control strategy including free and assistive modes in the exoskeleton. Finally, we conduct test bench and EMG experiments to validate the exoskeleton's mechanical performance and assistive effectiveness. The results demonstrate the outstanding performance of the mechanical system, free mode and personalized assistance.

Future works will focus on adaptive adjustment of assistance levels. We will investigate the adaptive assistance algorithm for more realistic and complex overhead tasks. In addition, our attention will be directed toward the real-time adjustment of the peak assistive torque angle, with potential solutions including the design of a novel mechanism or the addition of a remote drive unit.

REFERENCES

[1] A. Cieza et al., "Global estimates of the need for rehabilitation based on the global burden of disease study 2019: A systematic analysis for the global burden of disease study 2019," *Lancet*, vol. 396, no. 10267, pp. 2006–2017, Dec. 2020.

[2] X. Wang et al., "Work-related musculoskeletal disorders among construction workers in the United States from 1992 to 2014," *Occup. Environ. Med.*, vol. 74, no. 5, pp. 374–380, Apr. 2017.

[3] A. Ojelade et al., "Three passive arm-support exoskeletons have inconsistent effects on muscle activity, posture, and perceived exertion during diverse simulated pseudo-static overhead nutrunning tasks," *Appl. Ergonom.*, vol. 110, Jul. 2023, Art. no. 104015.

[4] J. K. Sluiter et al., "Criteria document for evaluating the work-relatedness of upper-extremity musculoskeletal disorders," *Scand. J. Work Environ. Health*, vol. 27, no. 1, pp. 1–102, 2001.

[5] J. Howard, V. V. Murashov, B. D. Lowe, and M.-L. Lu, "Industrial exoskeletons: Need for intervention effectiveness research," *Amer. J. Ind. Med.*, vol. 63, no. 3, pp. 201–208, Mar. 2020.

[6] J. Tian et al., "A systematic review of occupational shoulder exoskeletons for industrial use: Mechanism design, actuators, control, and evaluation aspects," *Actuators*, vol. 13, Dec. 2024, Art. no. 501.

[7] S. DeBock et al., "Passive shoulder exoskeleton support partially mitigates fatigue-induced effects in overhead work," *Appl. Ergonom.*, vol. 106, Jan. 2023, Art. no. 103903.

[8] Z. Du et al., "Development and experimental validation of a passive exoskeletal vest," *IEEE Trans. Neural. Syst. Rehabil. Eng.*, vol. 30, pp. 1941–1950, 2022.

[9] P. Maurice et al., "Objective and subjective effects of a passive exoskeleton on overhead work," *IEEE Trans. Neural. Syst. Rehabil. Eng.*, vol. 28, no. 1, pp. 152–164, Jan. 2020.

[10] G. Vazzoler, P. Bilancia, G. Berselli, M. Fontana, and A. Frisoli, "Analysis and preliminary design of a passive upper limb exoskeleton," *IEEE Trans. Med. Robot. Bionics*, vol. 4, no. 3, pp. 558–569, Aug. 2022.

[11] S. De Bock et al., "An occupational shoulder exoskeleton reduces muscle activity and fatigue during overhead work," *IEEE Trans. Biomed. Eng.*, vol. 69, no. 10, pp. 3008–3020, Oct. 2022.

[12] J. Kim,, J. Kim, Y. Jung, D. Lee, and J. Bae, "A passive upper limb exoskeleton with tilted and offset shoulder joints for assisting overhead tasks," *IEEE/ASME Trans. Mechatron.*, vol. 27, no. 6, pp. 4963–4973, Dec. 2022.

[13] A. van der Have, M. Rossini, C. Rodriguez-Guerrero, S. Van Rossom, and I. Jonkers, "The exo4work shoulder exoskeleton effectively reduces muscle and joint loading during simulated occupational tasks above shoulder height," *Appl. Ergonom.*, vol. 103, Sep. 2022, Art. no. 103800.

[14] L. Grazi, E. Trigili, G. Proface, F. Giovacchini, S. Crea, and N. Vitiello, "Design and experimental evaluation of a semi-passive upper-limb exoskeleton for workers with motorized tuning of assistance," *IEEE Trans. Neural. Syst. Rehabil. Eng.*, vol. 28, no. 10, pp. 2276–2285, Oct. 2020.

[15] H. Liu et al., "Implementation of a long-lasting, untethered, lightweight, upper limb exoskeleton," *IEEE/ASME Trans. Mechatron.*, vol. 30, no. 2, pp. 1345–1355, Apr. 2025.

[16] J. Tian et al., "A novel passive occupational shoulder exoskeleton with adjustable peak assistive torque angle for overhead tasks," *IEEE Trans. Biomed. Eng.*, vol. 72, no. 2, pp. 734–746, Feb. 2025.

[17] D. Park, S. Toxiri, G. Chini, C. D. Natali, D. G. Caldwell, and J. Ortiz, "Shoulder-sidewinder (shoulder-side wearable industrial ergonomic robot): Design and evaluation of shoulder wearable robot with mechanisms to compensate for joint misalignment," *IEEE Trans. Robot.*, vol. 38, no. 3, pp. 1460–1471, Jun. 2022.

[18] M. Rossini et al., "Design and evaluation of a passive cable-driven occupational shoulder exoskeleton," *IEEE Trans. Med. Robot. Bionics*, vol. 3, no. 4, pp. 1020–1031, Nov. 2021.

[19] S. Yu et al., "Design and control of a high-torque and highly backdrivable hybrid soft exoskeleton for knee injury prevention during squatting," *IEEE Robot. Autom. Lett.*, vol. 4, no. 4, pp. 4579–4586, Oct. 2019.

[20] D. A. Winter, *Biomechanics and Motor Control of Human Movement*. Hoboken, NJ, USA: Wiley, 2009.

[21] I. Pacifico et al., "An experimental evaluation of the proto-mate: A novel ergonomic upper-limb exoskeleton to reduce workers' physical strain," *IEEE Robot. Autom. Mag.*, vol. 27, no. 1, pp. 54–65, Mar. 2020.

[22] Y. Liu, "Report on nutrition and chronic disease status of Chinese residents (2020)," *China Food Nutr.*, vol. 26, no. 12, p. 2, 2020.

[23] H. J. Hermens et al., "Development of recommendations for SEMG sensors and sensor placement procedures," *J. Electromyography Kinesiology*, vol. 10, no. 5, pp. 361–374, Oct. 2000.

[24] S. Ding, F. Anaya-Reyes, A. Narayan, S. Ofori, S. Bhattacharya, and H. Yu, "A lightweight shoulder exoskeleton with a series elastic actuator for assisting overhead work," *IEEE/ASME Trans. Mechatron.*, vol. 29, no. 2, pp. 1030–1040, Apr. 2024.

[25] D. L. Waite, R. L. Brookham, and C. R. Dickerson, "On the suitability of using surface electrode placements to estimate muscle activity of the rotator cuff as recorded by intramuscular electrodes," *J. Electromyography Kinesiology*, vol. 20, no. 5, pp. 903–911, 2010.

[26] L. Van Engelhoven, N. Poon, H. Kazerooni, D. Rempel, A. Barr, and C. Harris-Adamson, "Experimental evaluation of a shoulder-support exoskeleton for overhead work: Influences of peak torque amplitude, task, and tool mass," *IISE Trans. Occup. Ergonom. Hum. Factors*, vol. 7, no. 3-4, pp. 250–263, Jul. 2019.